Infrared Spectrum of Phosphoenol Pyruvate: Computational and Experimental Studies

ARTICLE *in* THE JOURNAL OF PHYSICAL CHEMISTRY A · MARCH 2009

Impact Factor: 2.69 · DOI: 10.1021/jp809638u · Source: PubMed

Infrared Spectrum of Phosphoenol Pyruvate: Computational and Experimental Studies

Maria E. Rudbeck,*,† Saroj Kumar,† Maria-Andrea Mroginski,‡ Sten O. Nilsson Lill,§ Margareta R. A. Blomberg,§ and Andreas Barth*,†

Department of Biochemistry and Biophysics, The Arrhenius Laboratories for Natural Sciences, Stockholm University, SE-106 91 Stockholm, Sweden, Institut für Chemie, Max-Volmer-Laboratorium, TU Berlin, PC 14, Straβe des 17. Juni 135, D-10623 Berlin, Germany, and Department of Physics, Albanova, and Department of Biochemistry and Biophysics, The Arrhenius Laboratories for Natural Sciences, Stockholm University, SE-106 91 Stockholm, Sweden

Received: October 31, 2008; Revised Manuscript Received: January 16, 2009

The infrared spectrum of phosphoenol pyruvate (PEP) in aqueous solution was studied experimentally and theoretically in its fully ionized, singly protonated and doubly protonated form. The density functional theory with the B3LYP functional and with the 6-31G(d,p), 6-31++G(d,p), and 6-311++G(d,p) basis sets were used in the theoretical study. The calculations with the two latter basis sets and the CPCM continuum model for water showed good agreement with the experiments except for vibrations assigned to hydroxyl groups. These needed to be modeled with explicit water molecules. The effects of deuteration and of $^{13}C_{2,3}$ labeling of PEP were reproduced by the calculations.

Introduction

Glycolysis is a sequence of reactions which converts glucose to pyruvate and which produces small amounts of ATP. The final step is catalyzed by the enzyme pyruvate kinase (PK) and is a substrate-level phosphorylation step, forming pyruvate from phospoenol pyruvate (PEP); see Figure 1. Transfer reactions of phosphate groups from phosphate esters, such as PEP, play a fundamental role in biological processes including metabolism, cell signaling and regulation.[1−3]

Infrared spectroscopy is a powerful method to obtain information about the structure and function of molecules. It is used to provide information on several different properties such as bond lengths, bond strengths, protonation states, hydrogen bonding, and conformational changes. Assigning experimentally observed absorption bands to vibrational modes is not always straightforward, and usually several strategies are needed, for example, a combination of computational and experimental studies. Using quantum mechanical methods to calculate frequencies and intensities in order to assign the experimentally observed absorption bands to particular vibrations is today a widespread method. The calculated results can be further analyzed, regarding the composition of each normal mode, for example by animated atomic motion or by calculating the potential energy distribution (PED) of each normal mode.

Previously, computational and experimental studies have been performed on both the product pyruvate[4−7] and on other monoester phosphates, especially dimethyl phosphate.[8−13] Regarding PEP, the influence of hydrogen bonding between its phosphate group and water has been investigated;[14] however, that study focused on the phosphate group and did for example not include vibrational data for the carboxyl group. The chemical reactivity of the C3 atom of PEP has computationally been studied in terms of the hard−soft acid−base principle in enzymatic catalysis.[15] The study indicates that enzymes can control the reactivity by conformational changes of PEP.

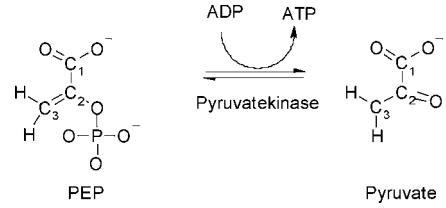

Figure 1. Reaction of PEP to pyruvate catalyzed by PK.

Despite the biological importance of PEP, no comprehensive theoretical study of the infrared spectrum seems to have been published. As a consequence, assignments of experimental spectra have to be based on common knowledge of group frequencies, a strategy which does not take into account the possible vibrational coupling between the carboxyl group, the phosphate group, and the carbon−carbon double bond, which are all in close proximity in PEP.

While experimental vibrational frequencies can be determined with wavenumber accuracy, quantum mechanical methods generally overestimate the frequencies. One source of error is the neglect of anharmonicity. Another problem in calculations is how to model the solvent effects. Today a common method is to use implicit solvent models, i.e., to represent the solvent as a bulk medium. Here, the self-consistent reaction field (SCRF) method is used which describes the solvent as a polarizable medium with a dielectric constant, ε. However, such models do not include localized hydrogen bonds between the solvent and the solute and may thereby neglect these important short-range interactions. These effects can be modeled by including explicit solvent molecules in the first solvation shell, a strategy which involves new problems such as the determination of the number and the orientation of the solvent molecules and also the treatment of many more local energy minima.[16] Furthermore, calculations including a larger number of explicit solvent molecules will become prohibitively costly.[16]

* To whom correspondence should be addressed. E-mail: maria.rudbeck@dbb.su.se (M.E.R.); andreas.barth@dbb.su.se (A.B.).

† Department of Biochemistry and Biophysics, The Arrhenius Laboratories for Natural Sciences, Stockholm University.

‡ Institut für Chemie, Max-Volmer-Laboratorium.

§ Department of Physics, Albanova, and Department of Biochemistry and Biophysics, The Arrhenius Laboratories for Natural Sciences, Stockholm University.

10.1021/jp809638u CCC: $40.75
Published on Web 02/20/2009

In this study the IR spectrum of PEP was studied both experimentally and computationally for three different ionization states: fully ionized, singly protonated, and doubly protonated. The article will discuss the choice of basis set and solvent effects. Furthermore, the assignments of the different experimental bands of PEP will be discussed in detail.

Materials and Methods

Experimental Details. The monopotassium salt of unlabeled PEP was purchased from Sigma, labeled PEP from Cambridge Isotopes Laboratories, and deuterium oxide (99.9 atom % D) from Sigma-Aldrich.

FTIR spectra were recorded at 4 cm^{-1} resolution on a Bruker Vertex 70 FTIR spectrometer equipped with a MCT detector. 50 mM labeled and unlabeled PEP in ^1H_2O and in ^2H_2O were measured at different pH values. The PEP sample was placed on a diamond ATR reflection element and the sample spectrum (200 scans) was ratioed against a 500 scan background spectrum.

Computational Details. All calculations were performed with the GAUSSIAN 03 program.[17] Both gas-phase and solvent geometries were optimized using density functional theory (DFT) with the B3LYP functional[18,19] and with three different basis sets: 6-31G(d,p), 6-31++G(d,p), and 6-311++G(d,p). 6-31G(d,p) and 6-31++G(d,p) are double-ζ basis sets with polarization functions for all atoms, the double + indicates that there are diffuse functions for all atoms. 6-311++G(d,p) is a triple-ζ basis set with both polarization and diffuse functions for all atoms. To find the most favorable conformations, the geometry optimization was performed on several different starting structures in the gas phase. They were generated by rotating three different dihedral angles (O−C_1−C_2−O, C_1−C_2−O−P, and C_2−O−P−O) with 30° interval in the range from 0 to 180°. In addition, for the fully ionized PEP the O−C1−C2−O angles were fixed at 0, 30, 50, 70, and 90° since no energy minima were found for these conformations. The purpose was to analyze whether an enzymatic control of PEP's conformation, as previously proposed,[15] can be detected by infrared spectroscopy.

The solvent effects were taken into account using a self-consistent polarized model (PCM), more specifically the conductorlike screening model (CPCM),[20,21] with the default values for water (dielectric constant, $\epsilon = 78.39$). For some of the structures, the solvent effect was described both implicitly and explicitly by using both the CPCM model and four explicit water molecules. Three water molecules were put to surround the phosphate and one water molecule was hydrogen bonded to the carboxyl group. No investigation was performed to find the global minima, i.e., the optimizations represent local minima and the energies can therefore not be compared.

Because of SCF convergence problems for some of the systems including the solvent model, parameters different from standard values were employed. First, the SCF=novaracc keyword was used in order to obtain a more strict SCF convergence. Second, the opt=gdiis option was chosen, which is the recommended algorithm for the geometry optimization of large systems and when molecules with flat potential energy surfaces are studied.[17]

The vibrational frequencies and the infrared absorbance were calculated for the optimized geometries; no scaling factors were applied. The calculations were performed using the same method and basis set as the optimization. All frequencies were analyzed using the ChemCraft program[22] and a PED program.[23]

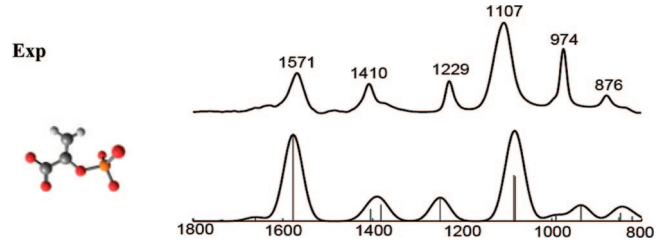

Figure 2. The infrared spectrum of fully ionized (FI) PEP. The top panel shows the experimental spectrum at pH 9, and the lower panel shows the computed spectrum using B3LYP/6-31++G(d,p). The computation included the CPCM to simulate the solvent effects.

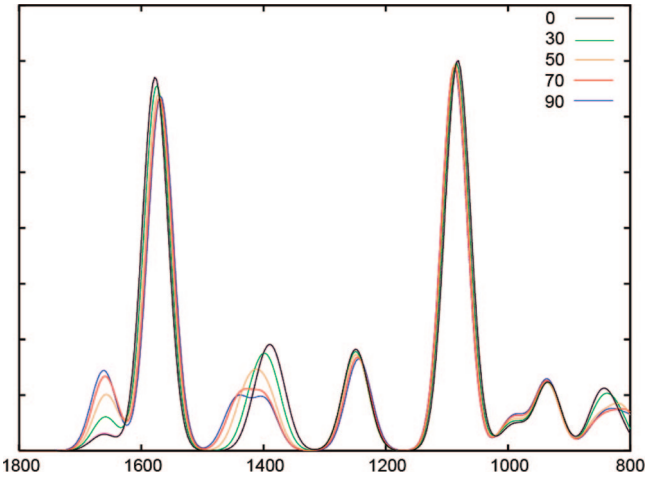

Figure 3. The computed infrared spectrum of FI-PEP during rotation of the dihedral angle O−C_1−C_2−O. The angle is frozen for all the calculations except for when the angle is 0°.

Results

We studied PEP in the gas phase by computation and in aqueous solution by computation and experiment. To model experiments in ^2H_2O, hydroxyl-deuterated PEP was also examined theoretically. In addition, $^{13}C_{2,3}$-labeled PEP was studied to clarify some of the band assignments. The experimental and computational results in water are reported in the main text, while a complete compilation of the experimental spectra (Figures S1−S3 of Supporting Information), a comparison of the calculations with the different basis sets for gas-phase calculations (Figures S4−S6 of Supporting Information) and for all CPCM-continuum calculations (Figures S7−S9 of Supporting Information), and the isotope effects on both the experimental and calculated spectra in water (Figures S10 and S11 of Supporting Information) can be found in the Supporting Information.

Comparison of Basis Sets. We studied several structures of PEP in three different ionization states. The infrared spectra for all conformations were computed using three different basis sets: 6-31G(d,p), 6-31++G(d,p), and 6-311++G(d,p). Figures 2,4−6 show the calculations with the 6-31++G(d,p) basis set and the CPCM-continuum. Figures S7−S9 of Supporting Information show the remaining results of these calculations using the CPCM continuum and the corresponding experimental spectra. For all protonation states the infrared spectra computed with the two basis sets including the diffuse functions are almost identical and close to experimental values, while the frequencies computed using the 6-31G(d,p) basis set are often overestimated compared to the experiment and higher than for the larger basis sets. In other words, for the three basis sets studied, the vibrational frequencies shift to lower values with larger basis

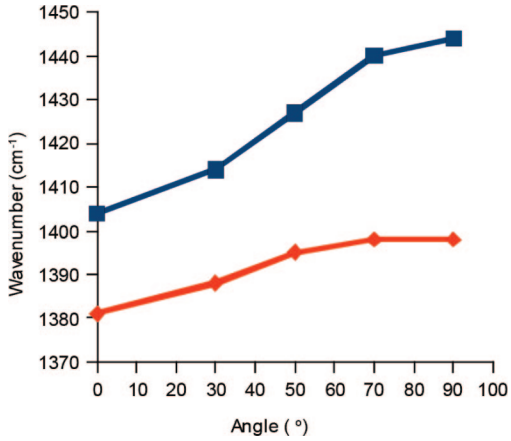

Figure 4. The relation between the two modes of FI-PEP which represent the 1410 cm^{-1} band. As the $O-C_1-C_2-O$ dihedral angle increases, the band gap increases.

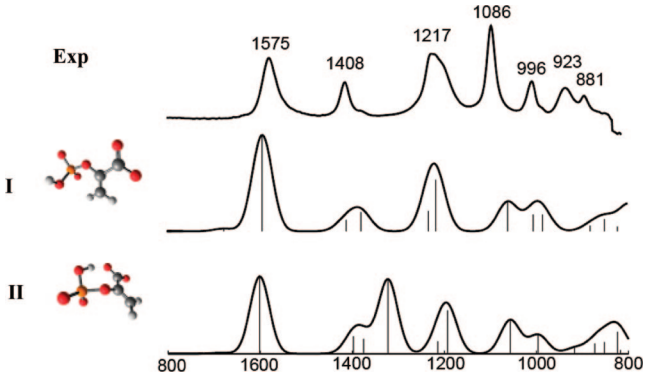

Figure 5. The infrared spectra of singly protonated phosphoenol pyruvate (SP-PEP). The top panel shows the experimental spectrum at pH 4. The middle panes shows the computed spectrum of structure I and the lower panel that of structure II. All computations are performed using B3LYP/6-31++G(d,p) and included the CPCM to simulate the solvent effects.

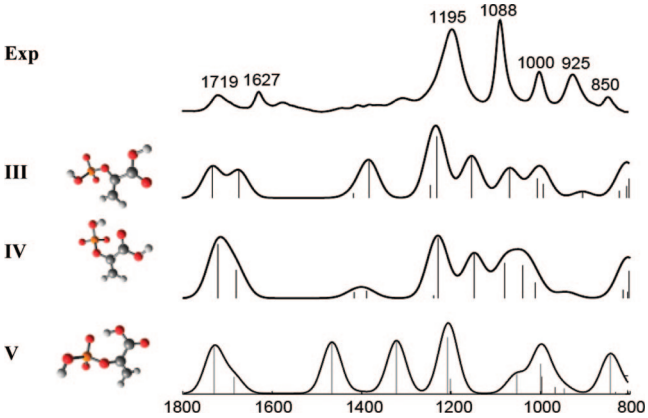

Figure 6. The infrared spectra of doubly protonated phosphoenol pyruvate (DP-PEP). The top panel shows the experimental spectrum at pH 2.1. All structures are computed using B3LYP/6-31++G(d,p) with the CPCM to simulate the solvent effects.

sets. For the fully ionized PEP, the root-mean-square deviation between calculation with CPCM-continuum and experiment in aqueous solution is 41 cm^{-1} for the 6-31G(d,p) basis set and 25 and 27 cm^{-1} for the 6-31++G(d,p) and 6-311++G(d,p) basis sets, respectively. Therefore, the results described below are those obtained with the 6−31++G(d,p) basis set.

Solvent Effects. The effects of the CPCM continuum were quantified for fully ionized PEP. The spectrum was computed using B3LYP/6-31++G(d,p) for both the gas phase and with the CPCM-continuum; the results are given in Table 1 for the CPCM-continuum. Both results can be found in Table S3 of Supporting Information. The root-mean-square deviation between the calculation with the 6-31++G(d,p) basis set, and the experiment is 38 cm^{-1} for the calculation in gas phase and 25 cm^{-1} with the CPCM-continuum. Thus the continuum model has a significant effect on the spectra and improves the agreement with experimental results. The results described below are therefore calculated using B3LYP/6-31++G(d,p) with the CPCM-continuum.

TABLE 1: Assignments and PEDs for FI-PEP Calculated with B3LYP/6-31++G(d,p) and CPCM Continuum[a]

experimental $\tilde{\nu}/cm^{-1}$		calculated normal modes of PEP (^1H_2O)			
PEP (^1H_2O)	[$^{13}C_{2,3}$]PEP (^1H_2O)	$\tilde{\nu}/cm^{-1}$	RA	assignment	PED (%)[b]
		1661	62	C2═C3 STRE	68
1571	1589/1557[c]	1577	1340	COO^- STRE	90
1410	1401	1404	185	CH_2 SCIS	60
1410	1401	1381	257	COO^- STRE	45
				CH_2 SCIS	23
1229	1206	1249	365	C−O(P) STRE	31
				CH_2 ROCK	26
1107	1106	1085	712	P−O STRE	99
1107	1106	1081	694	P−O STRE	98
∼980 sh		991	92	C−O(P) STRE	36
				CH_2 ROCK	42
974	972	935	245	P−O STRE	93
		850	60	CH_2 WAG	74
876	875	847	128	C1−C2 STRE	30
876	875			COO^- SCIS	34
		820	77	COO^- WAG	61

[a] The wavenumber, $\tilde{\nu}$, is given for the experimental data (PEP and [$^{13}C_{2,3}$]PEP in ^1H_2O) at pH 10 and for the computational data. Values in ^2H_2O are not included because none of the protons of FI-PEP will exchange for deuterium and the observed experimental band positions were very similar. RA, relative absorbance; STRE, stretching; SCIS, scissoring; ROCK, rocking; WAG, wagging; sh, shoulder. [b] Internal coordinates with a PED contribution of 15% or more are listed. [c] Band splits into two bands upon isotopic labeling.

FI-PEP. The chemical structure and the experimental and theoretical spectra for FI-PEP (pH = 9) are shown in Figure 2. Structural details of the energy minimized conformation are compiled in Table S2 of Supporting Information. The spectrum includes 6 distinct bands, the assignments of which are compiled in Table 1. At 1571 and 1410 cm^{-1}, the antisymmetric and the symmetric stretching vibrations of COO^- are observed, respectively. The calculations reveal that the symmetric stretching vibration is coupled to the scissoring (in plane bending) vibration of CH_2. The absorption at 1410 cm^{-1} includes an additional normal mode to which CH_2 scissoring contributes strongly.

Figure 3 shows the theoretical spectra of FI-PEP during the rotation of the dihedral angle O−C1−C2−O. The spectra show that the two modes that contribute to the 1410 cm^{-1} band are the only bands that significantly shift in frequency during the rotation. The changes in molecular energy and the vibrational frequencies are listed in Table 2. Figure 4 shows that the frequencies of both modes are higher when the angle increases from 0 to 90° and that the band gap between the two vibrations increases at larger angles. Another characteristic which appears during the rotation is the stronger absorption of the C═C stretching vibration at ∼1600 cm^{-1}.

The band at 1229 cm^{-1} is caused by a normal mode that has contributions from several internal coordinates, mainly from the C−O stretching vibration of the C−O−P group, here abbrevi-

TABLE 2: Conformational Dependency of Selected Vibrational Frequencies of FI-PEP with Energies and Frequencies Calculated with B3LYP/6-31++G(d,p) and the CPCM Continuum

angles[a]	relative energy (kJ/mol)	vibration 1[b] (cm^{-1})	vibration 2[b] (cm^{-1})
nonfrozen 0°	0	1404	1381
30°	1.35	1414	1388
50°	4.01	1427	1395
70°	7.08	1440	1398
90°	8.09	1444	1398

[a] The angle between C=C and COO^-. [b] The computed frequencies of the modes that constitute the experimental band at 1410 cm^{-1}.

ated C−O(P), and the rocking vibration of CH_2. The asymmetric and symmetric PO_3^{2-} stretching vibrations absorb at 1107 and 974 cm^{-1}, respectively. The small shoulder at the high wavenumber side of the 974 cm^{-1} band is likely caused by a normal mode involving the C−O(P) stretching vibration and the CH_2 rocking vibration. The band at 876 cm^{-1} is a superposition of two bands that are caused by the wagging vibration of the methylene and the C1−C2 stretching vibration coupled to the scissoring of the carboxylate group. Of the two bands, only the former is shifted in the calculation with isotopic-labeled [$^{13}C_{2,3}$]PEP. This explains why there is only a small shift in the experimental [$^{13}C_{2,3}$]PEP spectrum; see Table 1 (and Figure S3 of Supporting Information).

Singly Protonated (SP) PEP. The pK_a values of carboxylate and phosphate groups at pH 4.6 indicate that for the SP-PEP, the hydrogen atom is positioned on the phosphate group. This is also inferred from the experimental infrared spectra, see Figure 5, where the carboxylate bands (1575 and 1408 cm^{-1}) are still observed at pH 4.6, while the bands of the ionized phosphate group (1107 and 974 cm^{-1}) are no longer present. SP-PEP can adopt many conformations with local minima but two conformations are energetically more favorable. Their spectra are shown in Figure 5, their energies are given in Table S1 of Supporting Information and their structural details in Table S2 of Supporting Information. Conformation I has an extended form because of the repulsion from the negatively charged carboxylate and phosphate groups. Conformation II exhibits an internal hydrogen bond between the phosphate hydroxyl group and one of the oxygens of the carboxyl group. Conformer II was energetically favorable by 11 kJ/mol, when the solvent effects were modeled implicitly with the CPCM model. In aqueous solution, conformer I is expected to be better stabilized, compared to conformer II, by the hydrogen bonds from water molecules and by the minimized electrostatic repulsion in the extended conformation. The relative energies of the models with four explicit water molecules (and the CPCM model) are listed in Table S1 in the Supporting Information; however, it should be mentioned that these energies should not be directly compared since global minima were not obtained.

The calculated spectra for the two conformations are similar (see Figure 5). The assignments are listed in Table 3. An exception is that conformer II with the internal hydrogen bond has an extra vibration at 1322 cm^{-1}, with a strong absorption coefficient. This normal mode is caused by the POH in-plane-bending vibration and is upshifted by 317 cm^{-1} compared to the structure without the internal hydrogen bond. It is also the only case where the two basis sets with diffuse functions give very different frequencies - the difference is 32 cm^{-1} for conformer II.

As indicated by this large difference between the two conformers, the vibrational frequency of the POH in-plane-bending vibration is very sensitive to hydrogen bonding. Therefore, we studied whether this vibration in the extended structure I is affected by explicit water molecules in the calculation. The molecule was reoptimized with four explicit water molecules (also including the CPCM model). Indeed, placing hydrogen bonded water molecules close to the hydroxyl hydrogen and to the two unprotonated terminal oxygens of the phosphate group, shifted the POH bending vibration from 1005 up to 1164 cm^{-1}. Because of the sensitivity of this vibration to hydrogen bonding, it will cause a broadband in the experimental spectrum that we expect to contribute to the band at ∼1200 cm^{-1}, which is in agreement with Chapman et al.'s[24] experimental infrared study of orthophosphates. In line with this assignment, the low wavenumber shoulder of the 1217 cm^{-1} band in ^1H_2O is missing in ^2H_2O (see Figure S10 of Supporting Information). The calculated POH bending frequency shifts to the 900 cm^{-1} region upon deuteration which is consistent with reference.[24] A similar upshift of the POH-bending vibration, as for conformer I after including the explicit water molecules, can also be seen for conformer II. The POH-bending vibration is calculated at 1322 cm^{-1} without the explicit water molecules for the SP-PEP but appears at ∼1360 cm^{-1} when the water molecules are included. This upshift excludes that the POH-bending vibration contributes to the experimental absorption at ∼1200 cm^{-1}. The vibration can neither contribute to the experimental absorption at 1410 cm^{-1} since the experimental spectrum of SP-PEP (Figure 5) is very similar to that of FI-PEP (Figure 2) in this region. In SP-PEP there is no POH-bending vibration because the phosphate group is unprotonated. Therefore, the POH-bending vibration of conformer II does not seem to be observed in the experimental spectrum and we conclude that conformation II is little populated in aqueous solution.

Apart from the POH bending vibration, two additional normal modes contribute to the absorption at ∼1200 cm^{-1}, one consists of the C−O(P) stretching and CH_2 rocking vibrations and the other is attributed to the antisymmetric PO_2^- stretching vibration. The bands at 1577 and 1408 cm^{-1} are assigned to the antisymmetric and symmetric stretching vibration of COO^-, respectively, and the computations show that the second band includes a further mode dominated by the CH_2 scissoring vibration as also found for FI-PEP. The band at 1086 cm^{-1} is assigned to the symmetric PO_2^- stretching vibration while the band at 996 cm^{-1} arises from the coupling between C−O(P) stretching and CH_2 rocking vibrations. The small shoulder on the low wavenumber side of the 996 cm^{-1} band is the residual 974 cm^{-1} band for FI-PEP (see Figure 2), indicating that a small proportion of PEP remains unprotonated at pH 4.6. The small bands at 923 and 881 cm^{-1} are not easily assigned from the computations when the solvent effects are only considered by a continuum model. To aid their assignment, SP-PEP with four explicit water molecules (and the CPCM model) was also analyzed. Almost all frequencies were in agreement with the model without the explicit water molecules except for the P−O(H) stretching vibration where both a large upshift from 794 to 851 cm^{-1} and a higher intensity was calculated. This vibration is therefore expected to contribute to the 923 cm^{-1} band. A second mode, CH_2 wagging, contributes additionally. The absorption at 880 cm^{-1} is linked to the C1−C2 stretching vibration as is the 876 cm^{-1} band of FI-PEP. This interpretation explains why the absorption of the 923 cm^{-1} band is relatively strong and why the band does not exist for FI-PEP. It also

TABLE 3: Assignments and PEDs for Singly Protonated (SP) PEP Calculated with B3LYP/6-31++G(d,p) and CPCM Continuum

experimental $\tilde{\upsilon}$ /cm^{-1}		structure I of PEP (^1H_2O)[a]				structure II of PEP (^1H_2O)[a]			
PEP (^1H_2O)	PEP (^2H_2O)	$\tilde{\upsilon}$/cm^{-1}	RA	assignment[e]	PED (%)[b]	$\tilde{\upsilon}$/cm^{-1}	RA	assignment[e]	PED (%)[b]
		1677	37	C2═C3 STRE	70	1686	12	C2═C3 STRE	73
1575	1584	1593	1287	COO^- STRE	91	1601	1033	COO^- STRE	87
1408	1408	1411	154	CH_2 SCIS	66	1398	234	CH_2 SCIS	56
								COO^- STRE	24
1408	1408	1379	260	COO^- STRE	54	1375	200	COO^- STRE	41
				CH_2 SCIS	19			CH_2 SCIS	29
						1322	990	POH BEND[c]	87
1217	1219	1232	272	C—O(P) STRE	29	1214	166	C—O(P) STRE	31
				CH_2 ROCK	29			CH_2 ROCK	29
1217	1219	1216	689	P—O STRE	91	1193	580	P—O STRE	96
1086	1088	1060	394	P—O STRE	90	1057	450	P—O STRE	97
1217	1219	1005	224	POH BEND[c]	84				
996	996	985	225	C—O(P) STRE	41	996	253	C—O(P) STRE	40
				CH_2 ROCK	37			CH_2 ROCK	38
923	919	881	77	CH_2 WAG	94	917	76	CH_2 WAG	96
						874	138	TORS O—P—O—H	91
881	879	850	162	C1—C2 STRE	33	853	156	C1—C2 STRE	25
				COO^- SCIS	23			COO^- SCIS	36
		822	66	COO^- WAG	70	818	51	COO^- WAG	69
923[d]	919[d]	794	333	P—O(H) STRE	90	824	293	P—O(H) STRE	86

[a] See Figure 5 for more information about the structures. [b] Internal coordinates with a PED contribution of 15% or more are listed. [c] See text for assignment of this vibration to a band in experimental spectrum. [d] This vibration is sensitive to hydrogen bonding (see text). The band assignment was based on a calculation with explicit water molecules. [e] RA, relative absorbance; STRE, stretching; SCIS, scissoring; ROCK, rocking; WAG, wagging; sh: shoulder.

explains why there is only a small shift for both bands in ^2H_2O (see Figure S2 of Supporting Information).

Doubly Protonated (DP) PEP. The experimental spectrum for DP-PEP at pH 2.1, see Figure 6, indicates that both the carboxyl and the phosphate groups are protonated since the bands of the carboxylate group (1577 and 1409 cm^{-1}) are no longer observed. For DP-PEP, three conformations were studied in both the gas phase and when the continuum model was included. One has an extended conformation (III), see Figure 6, and the hydrogen atom can be positioned on the different phosphate oxygens without considerable change in energy. The second and third conformations (IV and V) exhibit an internal hydrogen bond between the carboxyl and the phosphate group. The energies of all these conformations are very close to each other (within 7 kJ/mol) when solvent effects are included. The energies and bond lengths of the conformations are listed in Tables S1 and S2 of Supporting Information.

The calculated infrared spectra of the different conformations for DP-PEP are represented in Figure 6. The assignments for conformations III, IV, and V are given in Table 4. The band at 1719 cm^{-1} is assigned to the C═O stretching vibration and the 1627 cm^{-1} band to the C2═C3 stretching vibration. The small band near 1577 cm^{-1} is the residual absorption of the carboxylate group, indicating that this group is ionized in a small fraction of the molecules. Between 1600 and 1250 cm^{-1}, the experimental spectrum is featureless. In contrast, for structure III one and for structure V two strong absorption bands are calculated in this region and assigned to delocalized modes involving the COH group. For structure IV, only weakly absorbing bands are calculated. Because of the discrepancy between computation and experiment in this spectral region, we explored whether the COH modes are affected by hydrogen bonding to explicit water molecules. Figure 7 shows the spectra of DP-PEP modeled with both explicit water molecules and the CPCM continuum model. The explicit water molecules do not affect the mode of structure IV; the mode might therefore contribute to the small bands between 1500 and 1300 cm^{-1} in the experimental spectrum. However, the explicit waters slightly upshift the two bands of structure V. Since details of hydrogen bonding seem to have little effect on the bands of structure V, we expect two distinct strong bands around 1400 cm^{-1} for structure V. This is not observed, and we conclude that structure V is little populated in aqueous solution.

For structure III, the explicit water molecules cause a frequency downshift and intensity increase of the mode involving the COH group from 1382 to 1315 cm^{-1}. This strong shift indicates a high sensitivity toward hydrogen bonding and we expect therefore the experimental band to be broad. Since even the inclusion of explicit water molecules models the hydration effect incompletely (as found for SP-PEP) we expect the experimental absorption of structure III considerably lower than 1315 cm^{-1} and suggest that the COH mode contributes to the band near 1200 cm^{-1}.

Thus, the broadband at ~1200 cm^{-1} is an overlap of several normal modes. The mode compositions with the two different solvation models (with and without the explicit water molecules) are different; however they include the vibrations of the same internal coordinates: C—O(H) stretching, COH bending and C1—C2 stretching, C—O(P) stretching, CH_2 rocking and COH bending, the antisymmetric PO_2^- stretching, and POH bending (for structures III and V where this vibration is upshifted from around 1000 cm^{-1} when including the explicit water molecules) vibrations. That the broadband includes the POH and COH bending vibrations is supported by the fact that the experimental absorption at ~1200 cm^{-1} is reduced in ^2H_2O (see Figure S11 of Supporting Information). The COH contribution increases the intensity of this band and changes its shape in comparison with the corresponding band of SP-PEP. The band at 1088 cm^{-1} corresponds to the PO_2^- symmetric stretching vibration and the 1000 cm^{-1} band is attributed to a mode that couples C—O(P) stretching and CH_2 rocking vibrations.

As for SP-PEP, DP-PEP needs to be modeled with explicit water molecules in order to assign the bands at 925 and 850 cm^{-1}. For structure III, the 925 cm^{-1} band is again assigned to

TABLE 4: Assignments and PEDs for DP-PEP Calculated with B3LYP/6-31++G(d,p) and CPCM Continuum

experimental $\tilde{\nu}$/cm^{-1}			structure III[a]				structure IV[a]				structure V[a]			
PEP (^1H_2O)	PEP (^2H_2O)	[$^{13}C_{2,3}$]PEP (^1H_2O)	$\tilde{\nu}$/cm^{-1}	RA	assignment	PED (%)[b]	$\tilde{\nu}$/cm^{-1}	RA	assignment	PED (%)[b]	$\tilde{\nu}$/cm^{-1}	RA	assignment	PED (%)[b]
1719	1707	1719	1732	372	C═O STRE	79	1721	641	C—O STRE	72	1731	525	C—O STRE	73
1627	1635	1578	1673	325	C2═C3 STRE	68	1681	334	C2═C3 STRE	66	1687	188	C2═C3 STRE	70
											1466	580	COH BEND	85
			1417	56	CH_2 SCIS	83	1417	70	CH_2 SCIS	71	1401	20	CH_2 SCIS	83
1195 (III)[c]			1382	438	C—O(H) STRE	25	1389	87	C—O(H) STRE	24	1321	597	C—O(H) STRE	43
					C1—C2 STRE	19			C1—C2 STRE	16			C1—C2 STRE	22
					COH BEND	19								
1195	1208	1186	1245	153	C—O(P) STRE	22	1239	33	C—O(P) STRE	23				
					CH2 ROCK	21			CH2 ROCK	17				
					COH BEND	21			COH BEND	29				
1195	1208	1186	1231	730	P—O STRE	87	1229	711	P—O STRE	88	1206	635	P—O STRE	52
1195	1208	1186	1153	499	C—O(H) STRE	49	1148	531	C—O(H) STRE	49	1200	167	C—O(H) STRE	21
					COH BEND	43			COH BEND	36			P—O STRE	43
1088	1091	1088	1068	353	P—O STRE	90	1080	418	P—O STRE	53	1051	218	P—O STRE	66
													POH BEND	18
1195	1208	1186	1006	232	POH BEND	82	1040	390	P—O STRE	45	997	334	POH BEND	73
													P—O STRE	18
1000	996	995	993	164	C—O(P) STRE	37	1012	185	C—O(P) STRE	35	994	192	C—O(P) STRE	40
					CH_2 ROCK	39			CH_2 ROCK	45			CH_2 ROCK	38
											964	71	COO(H) WAG	86
925	925	925	905	76	CH_2 WAG	98	943	73	CH_2 WAG	98	943	58	CH_2 WAG	97
850	820	843	822	83	C1—C2 STRE	40	815	99	C1—C2 STRE	36	828	16	C1—C2 STRE	33
				15	C—O(H) STRE	15							CO_2 SCIS	15
850	820	843	806	140	COO(H) WAG	59	805	75	COO(H) WAG	57	800	39	COO(H) WAG	77
925[d]	927[d]	925[d]	801	228	P—O(H) STRE	80	802	322	P—O(H) STRE	83	840	430	P—O(H) STRE	88

[a] See Figure 6 for more information about the structures. [b] Internal coordinates with a PED contribution of 15% or more are listed. [c] See text. [d] This vibration is sensitive to hydrogen bonding (see text). The band assignment was based on the calculation with explicit water molecules.

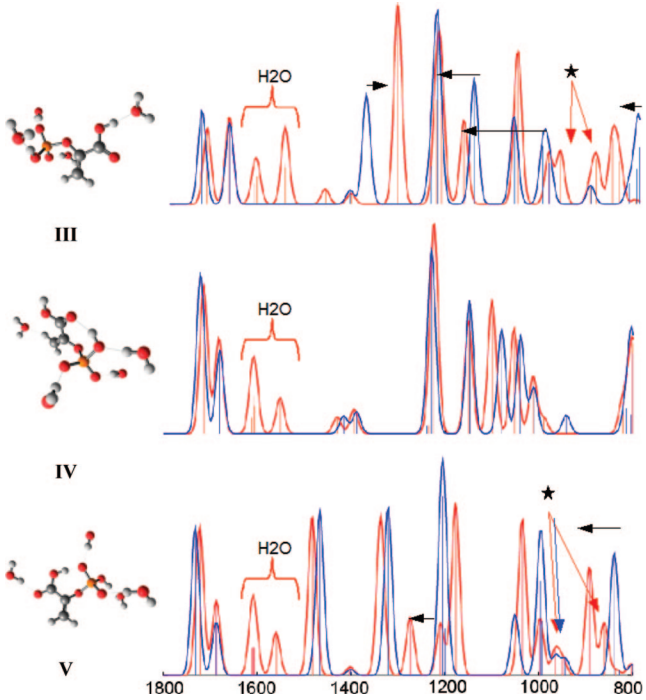

Figure 7. The calculated infrared spectra of DP-PEP. All structures are computed using B3LYP/6-31++G(d,p); the solvent effects are modeled with the CPCM and with explicit water molecules. Black arrows, from blue to red bands, indicate band shifts due to explicit water molecules. The stars indicate out-of-plane vibrations which are not observed in solution in the experimental spectrum.

the P—O(H) stretching vibration - after including the four explicit water molecules, see Figure 7, the vibration shifts up from 801 to 858 cm^{-1} (840 to 892 cm^{-1} for structure V). A second normal mode dominated by the CH_2 wagging vibration contributes to a small extent. The predominant contribution of the P—O(H) stretching vibration explains why the band is not affected by isotopic substitution in [$^{13}C_{2,3}$]PEP and hardly by deuteration (see Table 4 and Figure S3 of Supporting Information). For structure IV, a shift of the P—O(H) stretching vibration is not observed after including the explicit water molecules. It is calculated at 802 cm^{-1} and may give rise to an absorption below 800 cm^{-1}, which is outside the experimentally accessible spectral region. Therefore structure IV does not seem to contribute to the 925 cm^{-1} band. Since we have excluded structure V as a major species above, we conclude that the 925 cm^{-1} band is due to conformation III, which is therefore significantly populated in aqueous solution. The band at 850 cm^{-1} is assigned to the C1—C2 stretching vibration coupled to the C—O(H) stretching vibration and is downshifted compared to FI-PEP and SP-PEP in both experiment and calculation due to the protonation of the carboxyl group. This assignment also explains why the 850 cm^{-1} band shifts for both ^2H_2O and [$^{13}C_{2,3}$]PEP; see Table 4.

For all computations of SP-PEP and DP-PEP with explicit water molecules there are additional normal modes in the spectral range from 1800 to 800 cm^{-1}. They were not discussed above because they were not present in the spectra calculated with only the continuum model. For structure III, these additional modes are the POH and COH out-of-plane bending vibrations calculated at 892 and 969 cm^{-1}, respectively. They are expected to have considerably lower frequency after deuteration. Such band shifts are however not observed in the experimental spectra (compare Figures S1 and S2 in Supporting Information). This is in accordance with the literature, which describes the out-of-plane bending bands as very broad, due to many different relative orientations of interacting water molecules, and only visible in gas phase.[25−27]

Discussion

We calculated the infrared spectrum of PEP in three different protonation states using B3LYP with the three different basis sets 6-31G(d,p), 6-31++G(d,p), and 6-311++G(d,p) and together with the CPCM continuum model. Some structural models also included explicit water molecules in addition to the continuum model. The two larger basis sets show significant improvement of the calculated frequencies. For all protonation states the two spectra computed with basis sets including the diffuse functions are almost identical, and one can therefore conclude that the 6-31++G(d,p) basis set is sufficient for these molecular systems. Larger basis sets than 6-31G(d,p) are generally needed to describe the electronic structure of anions.[28,29]

One source of error in the quantum chemical calculations of vibrational frequencies is the neglect of anharmonicity effects. The calculated frequencies are therefore typically larger than those experimentally observed, however larger basis sets tend to yield better results.[30,31] According to Figures S7−S9 of Supporting Information, the B3LYP/6-31G(d,p) method generally overestimates the vibrational frequencies. For the larger basis sets, frequencies higher than 1200 cm^{-1} are often overestimated, while the frequencies below 1200 cm^{-1} are generally underestimated. Most vibrational frequencies are just slightly over- or underestimated (<3%); some are strongly affected by hydrogen bonding, as discussed below, and deviate up to 15% from experimental values.

A common technique to improve the agreement between the calculated frequencies and measured spectra is to use different scaling methods. Scaling the frequencies uniformly would not be fully satisfactory since some vibrations are underestimated while others are overestimated in our unscaled computations. Another approach is to scale the force constants depending on the type of atom and type of vibration, the so-called scaled quantum mechanical (SQM) method.[11,12] Both Florián et al.[11] and Katsyuba et al.[12] have scaled the force factors for molecules including phosphorus after optimization with B3LYP/6-31G(d) and obtained frequencies that compare well with experiments for most vibrations. However, to the best of our knowledge, not all scaling factors are available in the literature for the protonated PEP structures, for example, for the P−O(H) stretching vibration, and since most vibrational frequencies are in agreement with the experimental results, we decided not to introduce scaling.

Another source of error is the difficulties in modeling the solvent. Previous studies show that the hydrogen bonding may effect both the vibrational frequencies and the infrared intensities.[32,33] In this study, a discrepancy between calculated and measured frequencies was observed for vibrations involving protonated groups, i.e., PO(H) and CO(H) stretching and bending vibrations. These frequencies turned out to be very sensitive to hydrogen bonding. Therefore, the structures were reoptimized after including explicit water molecules that were hydrogen bonded to the phosphate and to the carboxyl groups. The results (see Figure 7) reveal several interesting details. First the P−O(H) stretching vibration is upshifted by 50 cm^{-1} for structure III while the remaining terminal P−O stretching modes do not shift. Second, the POH in-plane bending mode upshifts more than 100 cm^{-1}. Third, the intensities for all vibrations become more consistent with the experimental results, for example, the intensity for the P−O(H) stretching vibration increases when the explicit water molecules are included.

The close proximity of a carboxyl, a phosphate group, and a C2═C3 double bond in PEP raises the question as to the extent of vibrational coupling between these groups. This is an important aspect for the interpretation of experimental spectra of this biomolecule, since these groups give rise to relatively strong absorption and are therefore experimentally observable in studies of the catalytic mechanism of enzymes that have PEP as a substrate. According to Tables 1, 3, and 4 many of the normal modes are due to the vibration of predominantly one internal coordinate, whereas others comprise several internal coordinates which are strongly coupled. Significant coupling occurs with vibrations of the CH_2 group. The CH_2 scissoring vibration couples to the symmetric COO^- stretching vibration and the CH_2 rocking vibration to the C−O(P) stretching vibration. However, there is little coupling between the carboxyl group, the phosphate group and the C2═C3 double bond, and the vibrations of these groups in PEP have similar frequencies as in other molecules. Information on these groups from other molecules can therefore also be applied to PEP.

Conclusions

This work reports a combined experimental and theoretical analysis of the vibrational modes of the important biomolecule PEP in water for three ionization states. An extended conformation is suggested to exist in aqueous solution for the singly and the doubly protonated ionization states. For these conformations, the computational frequencies are very close to the experimental ones which allowed a complete band assignment in the studied spectral range from 1800 to 800 cm^{-1}. Therefore, using the B3LYP method in combination with a double-ζ basis set with diffuse functions and CPCM continuum model provides a satisfactory description of most vibrations in aqueous solution. However, vibrations involving the hydroxyl group are very sensitive to hydrogen bonding and should be modeled with a few explicit water molecules present.

The O−C1−C2−O dihedral angle correlates with the chemical reactivity of PEP.[15] We have shown here that for the FI-PEP the two modes that contribute to the experimental band at 1410 cm^{-1} experience frequency shifts when the angle is rotated. Because of the shifts, the conformation of PEP bound to an enzyme can be assessed by infrared spectroscopy. This will give important insight into the enzymatic mechanism.

Acknowledgment. We are grateful to the Knut och Alice Wallenbergs Stiftelse for funding the infrared spectrometer, to Ventenskapsrådet for providing the running costs and to the Center of Biomembrane Research for a stipend to Maria Rudbeck in the initial phase of the project. We would also like to thank one of the reviewers for pointing us to reference 15.

Supporting Information Available: The relative energies and structural details of the minimized conformations, the experimental infrared spectra of PEP in ^1H_2O and ^2H_2O and of [$^{13}C_{2,3}$]PEP in ^1H_2O for the three protonation states of PEP. Furthermore, it includes the computational infrared spectra and the PED for FI-PEP, SP-PEP, and DP-PEP in gas phase, for hydroxyl-deuterated PEP, and for DP-PEP with four explicit water molecules. This material is available free of charge via the Internet at http://pubs.acs.org.

References and Notes

(1) Florián, J.; Warshel, A. *J. Am. Chem. Soc.* **1997**, *119*, 5473.
(2) Westheimer, F. *Science* **1987**, *235*, 1173.
(3) Knowles, J. *Ann. Rev. Biochem.* **1980**, *49*, 877.
(4) Duczmal, K.; Darowska, M.; Raczynska, E. *Vib. Spectrosc.* **2005**, *37*, 77.
(5) Kakkar, R.; Pathak, M.; Radhika, N. *Org. Biomol. Chem.* **2006**, *4*, 886.

(6) Reva, I.; Stepanian, S.; Adamowicz, L.; Fausto, R. *J. Phys. Chem. A* **2001**, *105*, 4773.
(7) Raczynska, E.; Duczmal, K.; Darowska, M. *Vib. Spectrosc.* **2005**, *39*, 37.
(8) Petrov, A. S.; Funseth-Smotzer, J; Pack, G. R. *Int. J. Quantum Chem.* **2005**, *102*, 645.
(9) Shimanouchi, T.; Tsuboi, M.; Kyogoku, Y. *Advances in Chemical Physics: Structure & Properties of Biomolecules*; Wiley Interscience: New York, 1964.
(10) Liang, C.; Ewig, C. S.; Stouch, T. R.; Hagler, A. T. *J. Am. Chem. Soc.* **1993**, *115*, 1537.
(11) Florian, J.; Baumruk, V.; Strajbl, M.; Bednarova, L.; Stepanek, J. *J. Phys. Chem.* **1996**, *100*, 1559.
(12) Katsyuba, S.; Vandyukova, E. *Chem. Phys. Lett.* **2003**, *377*, 658.
(13) Kang, N. S.; Jung, D. H.; No, K. T.; Jhon, M. S. *Chem. Phys. Lett.* **2002**, *364*, 580.
(14) Brandán, S. A.; Díaz, S. B.; López, J. J.; Disalvo, E. A.; Ben Altabef, A. *Spectrochim. Acta A* **2007**, *66*, 884.
(15) Li, Y.; Evans, J. *Proc. Natl. Acad. Sci. U.S.A.* **1996**, *93*, 4612.
(16) Cramer, C. J.; Truhlar, D. G. *Chem. Rev.* **1999**, *99*, 2161.
(17) Frisch, M. J.; Trucks, G. W.; Schlegel, H. B.; Scuseria, G. E.; Robb, M. A.; Cheeseman, J. R.; Montgomery, J. A., Jr.; Vreven, T.; Kudin, K. N.; Burant, J. C.; Millam, J. M.; Iyengar, S. S.; Tomasi, J.; Barone, V.; Mennucci, B.; Cossi, M.; Scalmani, G.; Rega, N.; Petersson, G. A.; Nakatsuji, H.; Hada, M.; Ehara, M.; Toyota, K.; Fukuda, R.; Hasegawa, J.; Ishida, M.; Nakajima, T.; Honda, Y.; Kitao, O.; Nakai, H.; Klene, M.; Li, X.; Knox, J. E.; Hratchian, H. P.; Cross, J. B.; Bakken, V.; Adamo, C.; Jaramillo, J.; Gomperts, R.; Stratmann, R. E.; Yazyev, O.; Austin, A. J.; Cammi, R.; Pomelli, C.; Ochterski, J. W.; Ayala, P. Y.; Morokuma, K.; Voth, G. A.; Salvador, P.; Dannenberg, J. J.; Zakrzewski, V. G.; Dapprich, S.; Daniels, A. D.; Strain, M. C.; Farkas, O.; Malick, D. K.; Rabuck, A. D.; Raghavachari, K.; Foresman, J. B.; Ortiz, J. V.; Cui, Q.; Baboul, A. G.; Clifford, S.; Cioslowski, J.; Stefanov, B. B.; Liu, G.; Liashenko, A.; Piskorz, P.; Komaromi, I.; Martin, R. L.; Fox, D. J.; Keith, T.; Al-Laham, M. A.; Peng, C. Y.; Nanayakkara, A.; Challacombe, M.; Gill, P. M. W.; Johnson, B.; Chen, W.; Wong, M. W.; Gonzalez, C.; Pople, J. A. *Gaussian 03*; Gaussian, Inc.: Wallingford, CT, 2004.
(18) Becke, A. D. *J. Chem. Phys.* **1993**, *98*, 5648.
(19) Lee, C.; Yang, W.; Parr, R. G. *Phys. Rev. B* **1988**, *37*, 785.
(20) Barone, V.; Cossi, M. *J. Phys. Chem. A* **1995**, *102* (1998), .
(21) Cossi, M.; Rega, N.; Scalmani, G.; Barone, V. *J. Comput. Chem.* **2003**, *24*, 669.
(22) http://www.chemcraftprog.com.
(23) Spies, M.; Smit, K.; Mroginski, M. A.; Mark, F. *GVA Program*, revision 2007; University of Duisburg and Max Planck Institut für Strahlenchemie.
(24) Chapman, A. C.; Thirlwell, L. E. *Spectrochim. Acta* **1964**, *20*, 937.
(25) Coates, J. *Interpretation of Infrared Spectra, A Practical Approach*; Meyers, R. A., Ed.; John Wiley & Sons Ltd: Chichester, 2000..
(26) Ostrowska, J.; Narebska, A. *Colloid Polym. Sci.* **1979**, *257*, 128.
(27) Colthup, N. B.; Daly, L. H.; Wimberley, S. E. *Introduction to Infrared and Raman Spectroscopy*; Academic Press: Boston, 1990.
(28) Rienstra-Kiracofe, J. C.; Tschumper, G. S.; Schaefer, H. F., III; Nandi, S.; Ellison, G. B. *Chem. Rev.* **2002**, *102*, 231.
(29) Millet, A.; Gimbert, Y.; Greene, A. E. *J. Comput. Chem.* **2006**, *27*, 157.
(30) Meier, R. J. *Vib. Spectrosc.* **2007**, *43*, 26.
(31) Merrick, J. P.; Moran, D.; Radom, L. *J. Phys. Chem. A* **2007**, *111*, 11683.
(32) Smets, J.; McCarthy, W.; Maes, G.; Adamowicz, L. *J. Mol. Struct.* **1999**, *476*, 27.
(33) Dimitrova, Y.; Daskalova, L. I. *THEOCHEM* **2007**, *823*, 65.

JP809638U